TECHNICAL RESEARCH REPORT

Fractal Geometry Applied to On-line Monitoring of Surface Finish

by G. Zhang and S. Gopalakrishnan

T.R. 94-64

INSTITUTE FOR SYSTEMS RESEARCH

Sponsored by
the National Science Foundation
Engineering Research Center Program,
the University of Maryland,
Harvard University,
and Industry

Fractal Geometry Applied to On-line Monitoring of Surface Finish

Guangming Zhang and Shivakumar Gopalakrishnan
Department of Mechanical Engineering and Institute for Systems Research
University of Maryland
College Park, MD 20742 USA

Abstract

Surface finish of machined parts determines the functionality of the product and also the machining requirements for making the parts. On-line monitoring of surface finish has been an active area of machining research. Conventional contact techniques used for surface finish measurement are not suitable for in-process measurement as they interfere with the machining operation. In this research, the principle of fractal geometry and image processing techniques are used to implement a practical area-based surface finish monitoring system. Fractal dimension estimated from the captured image is used to characterize the machined surface with success.

Nomenclature

a: scaling constant in W-M function

CCD: charge coupled device

CNC: computer numerical control

D: fractal dimension

ϕ_n :arbitrary phase in W-M function

g: scaling constant in W-M function

h: height variation along the trace

k: number of bits required to store an integer

m: counter used in the implemented algorithm

N: number of segments or boxes covering a given set

n: index used in W-M function

Ra: roughness average in µm

s: edge size of boxes

W-M: Weierstrass Mandelbrot function

x: Distance in mm

ε: magnification factor

1. INTRODUCTION

Computer integrated manufacturing requires fast and accurate systems that provide the feedback to control the machining process and improve product quality and productivity. On-line process monitoring has been an active area of research because it is recognized as an essential part of fully automated manufacturing systems. One of the parameters to be controlled in machining is surface finish, which is a vital criterion in the performance and utility of industrial products.

Literature survey reveals that existing surface roughness monitoring techniques can be mainly divided into two groups: optical and stylus profiling methods [1]. As a conventional method, stylus profiling is a contact measurement, which usually interferes with the machining operation and is not suitable for in-process applications [2]. Optical methods overcome many standard problems associated with stylus methods. The major limitation of the optical methods currently being used [3], such as laser profilometry, is that they scan the surface line by line and, thus, generate profiles. To completely characterize the surface texture, many measurements have to be taken repeatedly over an area. This procedure would be most effective for off-line measurements, but not for in-process measurements. In addition, laser profilometry methods require large and expensive equipment, causing difficulties in their implementation as on-line surface finish monitoring systems.

Pioneering research to use fractal geometry for characterizing machined surfaces was proposed by Majumdar, et al. in 1990 [4-6]. In their early work, profilometric measurements were taken from a machined surface, numerical values of a fractal parameter called fractal dimension were estimated and reconstruction of surface topographies was successfully completed. However, intensive computational requirements limit its use as an in-process surface finish monitoring system. Devoe and Zhang implemented a prototype system where a Charge Coupled Device (CCD) camera was used to capture surface images during machining, and statistical parameters using the mean and standard deviation of the captured image data were formulated to perform optical area-based surface quality assessment [7-8]. This approach made it possible to monitor the surface roughness as the surface was being machined. On the downside, the formulated parameters were sensitive to machining environmental conditions and required rigid calibration to obtain reliable results.

This paper presents a new technique to characterize machined surfaces. The technique applies fractal geometry to perform optical area-based surface quality assessment. A prototype system to implement in-process measurement using fractal geometry is designed. A system calibration is performed, prior to the machining operation, to establish the correspondence between the fractal dimension and the roughness average. During the machining operation, the system captures images of the part being machined using a CCD camera during the machining operation. Estimates of fractal dimension are calculated from the whole image data by a software program. Conversion from the fractal dimension to the roughness average is made instantly for the purpose of monitoring finish quality of the surface being machined. Important findings from this investigation are 1) a close correlation between the calculated area-based fractal dimension value and the measured roughness average value, and 2) the fractal parameter used in this research is less sensitive to changes in the ambient conditions when compared with other optical parameters. These findings indicate the capabilities and potential of the proposed fractal geometry-based technique in the development of future on-line monitoring systems.

The paper will first present the theoretical background and a brief introduction to fractal geometry. It is followed by the description of the designed prototype system and system calibration. Experimental results are discussed through an analysis of their implications to illustrate the effectiveness, as well as the limitations, of the prototype system in performing in-process assessment of surface finish during the machining operation.

2. BASIC METHODOLOGY

2.1 Fractal Geometry

Fractal geometry, as an extension of classical Euclidean geometry, characterizes the average slope of a profile in the two-dimension space and reflects the space filling ability in the three-dimension space. Fractal parameters have been used to accurately represent naturally occurring shapes like the profiles of mountains, surface profiles, clouds, leaves, etc., using a simple and compact set of equations [9]. Infinite numbers of fractional dimensions are permitted in fractal geometry as opposed to the three integer dimensions allowed in Euclidean geometry. Fractals are identified by their property of appearing similar to the original image under a range of magnification scales. In broad terms, a fractal is a rough or fragmented geometric shape that can be subdivided in parts, each of which is nearly a reduced copy of the whole. Fractals can be described by a scale invariant parameter called fractal dimension denoted by D. The fractal dimension is a measure of how densely the fractal occupies the space in which it lies.

As illustrated in Fig. 1a, a line of unit length can be broken into equal segments of length, $1/\varepsilon$. Each segment is similar to the original and needs a magnification of ε to be a replica of the original line. The number of such segments is $N=\varepsilon^1$. Similarly for a square having unit sides, a small square of side, $1/\varepsilon$, needs a magnification of ε to be a replica of the original unit square, as illustrated in Fig. 1b. The number of squares of side, $1/\varepsilon$, inside the unit square is $N= \varepsilon^2$. In a general sense, for an object of fractal dimension D, it can be said that

$$N = \varepsilon^D \quad (1)$$

Hence the fractal dimension of an object can be obtained by

$$D = \frac{\log N}{\log \varepsilon} \quad (2)$$

This definition of fractal dimension of an object is based on the object's self-similarity. Therefore, it is also called a similarity dimension. A classical example used to demonstrate non integer fractal dimensions is the Koch curve, as illustrated in Fig. 2. The Koch curve has a fractal dimension D = 1.26, which is a real number. The procedure for its construction is 1) a straight line is broken into three equal parts, 2) the middle part is removed and replaced with two segments of equal length such that it forms an equilateral triangle without a side, and 3) this process is carried out recursively on each straight length segment. Its fractal dimension can be calculated by the following:

$$D = \frac{\log N}{\log \varepsilon} = \frac{\log 4}{\log 3} = \frac{\log 4x4}{\log 3x3} = 1.26 \quad (3)$$

2.2 Fractal Geometry as Applied to Machined Surfaces

In this section, an intuitive explanation on how fractal geometry can be used to represent the surface roughness is given. As shown in Fig. 3, a line, which represents an ideal smooth surface profile, has a fractal dimension of 1. In general, a surface profile should have a fractal dimension ranging between one and two. Consequently, a filled square is the limit in which the surface profile essentially occupies the entire space and has a fractal dimension equal to two. Thus, it can be seen that as the surface becomes rougher the fractal dimension increases.

Using fractal geometry to characterize surface roughness provides a realistic representation of the machined surface. As an example, a surface profile obtained through measurement is shown in Fig. 4a. A portion is selected from the profile and magnified by, an equal factor, say 2.0, to both axes. As shown in Fig. 4b, the magnified portion does not look similar to the original profile. Instead, it looks like an elongated version of the original portion. If using different magnification scales on these axes, say 2.0 and 0.8, the magnified portion, which is shown in Fig. 4c, looks similar to the original profile. This property is known as self-affinity [10]. This property means that self-affine shapes are statistically invariant under transformations that magnify different coordinates by different scales [9]. Profiles taken from a machined surface can be treated as self-affine fractals.

The Weierstrass - Mandelbrot fractal function (W-M) was proposed by Mandelbrot to represent surface topography [11]. The relation between the variation of profile heights and the fractal dimension is defined as

$$h(x) = \sum_{n=-\infty}^{\infty} \frac{(1 - e^{(2\pi j a^n x + \phi_n)})}{a^{n(2-D)}} \qquad (4)$$

where a = constant, D = Fractal Dimension, ϕ_n = Arbitrary phases, $h(x)$ = Height variation along the surface

Mathematically, the W-M function is a continuous function everywhere , but nowhere differentiable. This is due to the fact that under different scales of magnification, more and more details of the roughness appear [12]. Consequently, the function is nowhere differentiable. It can be shown that the W-M function possesses the following relation [9]

$$h(gx) = g^{(2-D)} h(x) \qquad (5)$$

where g is the scaling factor for the x coordinate. Equation 5 indicates that the scaling factor of h(x), the height variation, is $g^{(2-D)}$. The two different scaling factors imply that the W-M function is self-affine. Figure 5 presents a comparison between a measured surface topography and a simulated surface topography using the W-M function. They look very similar to each other and possess similar properties of continuity and self-affinity.

3. SYSTEM IMPLEMENTATION AND EVALUATION

3.1 Design of a Prototype On-Line Monitoring System

The major objective of this research is to implement an on-line monitoring system using fractal geometry for an effective estimation of the finish quality of a surface being machined. The design of such a prototype system for a Computer Numerical Controlled (CNC) milling machining center is illustrated in Fig. 6a. The implementation of the prototype system is shown in Fig. 6b. The system consists of a CCD camera, a variable intensity light source, a fiber optic cable to orient the light, an attachment to hold the CCD camera and a computer system for data acquisition and analysis. During the operation, the surface being machined is illuminated by the variable intensity light source through the fiber optic cable. The image is picked up by the camera and sent to the computer through a frame grabber at a rate of 30 frames per second. These images are then analyzed to determine the fractal dimension of the captured surface texture.

In this research, a computer program was written to calculate fractal dimension from the area-based image data. It has several unique features. First, the fractal analysis is made over an area of the machined surface. Area-based assessments provide a better characterization of the surface topography. The second feature is the application of the box counting algorithm which sorts bits of the image bytes to speed up the calculation of fractal dimension [13]. The concept of the box counting algorithm is illustrated in Figs. 7a and 6b. Boxes are virtually constructed for a given edge size denoted by s, which varies from two to 2^k, where k is the number of bits required to store an integer (16 in our system). This parameter is the reciprocal of the parameter ε defined in Eq. 1. The counting procedure identifies those boxes containing the surface texture, say N boxes. This procedure starts with the edge size equal to 2^k, is repeated with decreasing edge size, and will be terminated when the edge size reaches its limiting value - two. The fractal dimension is determined by calculating the slope of the log(N) vs $\log(\frac{1}{s})$ plot using linear regression analysis. It should be noted that the ratio of log(N) to $\log(\frac{1}{s})$ may not provide useful information for the fractal dimension calculation when the box size is too small or too large. It would suffice that the fractal dimension is determined by identifying N for those median box sizes. This fact reduces the computational effort significantly and makes fast calculation of fractal dimension possible. Such a reduction in computation creates a unique opportunity for on-line monitoring systems to effectively assess the finish quality of a machined surface during the operation.

3.2 Calibration of the Prototype System

Prior to utilization of the prototype system, a calibration process was carried out to establish the correspondence between the fractal dimension determined by the prototype system and the roughness average, a parameter commonly used in practice. In this study, thirty-six aluminum specimens were prepared. They were machined out of 2" wide blocks using a four flute 3/4" diameter end mill. The depth of cut was kept at 1.27 mm. The feedrate and spindle speed varied from 25.4 to 66 mm/min and 800 to 1100 rpm, respectively. During these machining operations, numerical values of the fractal dimension were estimated and recorded on-line. After machining, surface profiles were taken from the machined surfaces using a stylus Talysurf profilometer. The roughness of each sample was determined from the average of five stylus traces over the full width of the milled path, to obtain the true surface roughness as the process used to machine the specimens was milling. Figure 8a is a plot of the calculated fractal dimension values vs the measured roughness average values. A curve fit was performed on the data plot. The best fit was found to be a third degree polynomial with a correlation coefficient of $R^2 = 0.85$. The equation of this calibration curve was given by

$$D= 2.228 + 0.131Ra + 0.0263Ra^2 - 0.0184Ra^3 \tag{6}$$

The obtained calibration curve clearly indicates that the fractal dimension is a measure of the surface roughness because fractal dimension increases its value as the roughness average value increases. Although deviations of data from the calibration curve are shown, a quantitative correlation between them exists, as given by Eq. 6.

3.3 Verification of the Prototype System

In order to verify capability of the implemented prototype system, a second set of thirty-six machining tests were carried out to repeat the machining tests performed during the calibration process. The workpiece material, the end mill cutter, and the machining conditions were kept as close to the previous ones as possible. During these machining operations, the thirty-six fractal dimension values were estimated on-line and converted to their corresponding roughness average values using the calibration curve, or based on the correlation given by Eq. 6. After machining, surface profiles were taken from the machined surfaces using a stylus Talysurf profilometer and the roughness readings of each sample were recorded during these measurements. A comparison was made between the converted, or calculated value, and the measured roughness average values, as illustrated in Fig. 8b. The plot shows a good agreement between the two sets of roughness average data. Evidently, deviations occur. The maximum error was 0.23 μm and the minimum error was 0.01 μm. The average error was 0.105 μm with a standard deviation of 0.122 μm. In general, the error level is acceptable considering the adverse conditions under which the system is operated. These deviations can be caused by a few factors. Among them are the variation of optical parameters such as ambient lighting and intensity of the light source, the variation of machining conditions such as the effect caused by the cutting mechanics on the surface texture formation during machining, variation among the roughness average measurements using a stylus surface profilometer, and the algorithm used to calculate the fractal dimension.

3.4 Sensitivity Analysis

The fractal dimension based prototype system is an optical system. Any practical on-line monitoring system must be stable under variation in the environmental conditions. To further verity its applicability, sensitivity analysis was performed to determine how the calculation of the fractal dimension was affected by variation of the image of the machined surface captured by the CCD camera. Four variables that were selected for the sensitivity study are listed:

(a) ambient lighting
(b) incident angle of the light source
(c) horizontal orientation of the light source with respect to the machining direction
(d) intensity of the light source

Effects of these factors on the system performance can be anticipated based on prior knowledge of the system and fractal geometry. For example, ambient light increases the brightness level of the pixels and thereby removes the surface detail. This makes the surface look rougher and thus will increase the fractal dimension. The variations in the incident angle and the horizontal orientation of the light source are expected to bring out more details or less details of the machined surface due to shadow effect, thus varying the fractal dimension. As the light source becomes more intense, the overall image becomes brighter and thus results in an increase of the mean value of all the pixels in the image. This again is expected to increase the fractal dimension.

A full factorial design methodology was employed to estimate the effect of these variables on the fractal dimension calculation [14]. Each of the four variables was set at two levels, as listed in Table 1. For example, a fixture was used to adjust the horizontal orientation and the incident angle of the light at two levels. The level light source intensity was varied by using two settings in the dial. The high level was set at the maximum position and the low level was set by reducing the light source brightness to 80% of the maximum setting. Ambient lighting was produced by nine 34W fluorescent bulbs placed between 1.5m to 3m overhead of the experimental arrangement. Sunlight was not allowed to reach the specimen. As a result, a total of sixteen tests, as a combination of the four variables at two levels, were performed off-line on a single specimen with a known surface roughness value. This procedure was repeated on four specimens with surface roughness values at 0.23, 0.36, 0.53, and 0.70 μm, respectively. Table 1 lists the 16x4 experimental data. Empirical models to represent the linear relation between the fractal dimension and the four variables are listed below.

For the specimen with Ra = 0.23 μm:

$$D = 2.220 + 0.013 \text{ [orientation of light source]} + 0.018 \text{ [incident angle of light]} + 0.025 \text{ [light source intensity]} + 0.070 \text{ [ambient lighting]} \quad (7)$$

For the specimen with Ra = 0.36 µm:

$$D = 2.292 + 0.028\ [\text{orientation of light source}] + 0.013\ [\text{incident angle of light}] + 0.026\ [\text{light source intensity}] + 0.030\ [\text{ambient lighting}] \quad (8)$$

For the specimen with Ra = 0.53 µm:

$$D = 2.341 + 0.031\ [\text{orientation of light source}] + 0.022\ [\text{incident angle of light}] + 0.029\ [\text{light source intensity}] + 0.050\ [\text{ambient lighting}] \quad (9)$$

For the specimen with Ra = 0.70 µm:

$$D = 2.418 + 0.038\ [\text{orientation of light source}] + 0.021\ [\text{incident angle of light}] + 0.026\ [\text{light source intensity}] + 0.030\ [\text{ambient lighting}] \quad (10)$$

Numerical values of the first item in these empirical models, namely 2.220, 2.292, 2.341 and 2.418, are the four column averages listed in Table 1. They characterize the general trend between the fractal dimension and the roughness average. Numerical values shown in the front of these four variables are coefficients to represent the effects of higher level settings on the fractal dimension calculation. For example, 0.013 in Eq. 7 implies the calculated fractal dimension will be increased by 0.013 when a higher level of the orientation of light source is used for capturing the image. Therefore, these coefficients serve as indications of the sensitivity of the fractal dimension to these four variables.

4. DISCUSSION OF RESULTS

4.1 Main Effects of the Four Variables on Fractal Dimension

Examining the coefficients in Eqs. 7-10, factors, such as ambient lighting, incident angle of the light source, horizontal orientation of the light source with respect to the machining direction, and intensity of the light source, have different effects on the determination of fractal dimension during machining. The results from the factorial design are analyzed below, in the order of their importance.

(a) Ambient Lighting (average level = 0.045)

The four coefficients associated with the ambient lighting variable in Eqs. 7-10 are 0.070, 0.030, 0.050, and 0.030, respectively. The average is 0.045, larger than the three other averages. This means that ambient lighting condition introduces the most variation in the fractal dimension calculation. This is due to the fact that increase in ambient light removes details of the machined surface and tends to increase the fractal dimension. Therefore it is very important that the prototype system should be calibrated under similar lighting conditions as expected during the actual machining.

(b) Source Light Intensity (average level = 0.027)

The next important variable is the intensity of the light source with the average level at 0.027. Similar to the variation in ambient light, increase in intensity of the light source may make the image more flat and thus the fractal dimension increases. But the light source intensity can be controlled during the operation rather easily. For small variations in the light source the fractal dimension is not expected to vary by a large amount.

(c) Horizontal orientation of light source (average level = 0.027)

Variation in orientation of the light source with respect to the machining direction varied the output at the average level of 0.027. This is very likely due to the anisotropic nature of the milled surface, which affects the shadow region in the captured image. The surface topography observed in the image may become clearer or more hidden according to the orientation of the light source. Note that this coefficient in Eq. 10 is 0.038 and is significantly larger than 0.013 in Eq. 7. This indicates that control of the shadow effect is very important for rough machining operations, and implies that the orientation of the CCD camera with respect to the machine tool motion should not vary during machining.

(d) Incident angle of the light source (average level = 0.018)

Under a confidence level of 95% this effect can be ignored for small variations in the incident angle. This may be due to the fact that slight variations in the incident angle do not affect the image to produce a measurable variation in the output. This fact makes the prototype system more applicable if the depth of cut is not constant and the resulted variation of the incident angle of the light source is small (less than 10^{o} in the current study). Under these circumstances, the light source need not be adjusted accordingly during machining.

4.2 Significant Finding

Results from this study clearly indicate that fractal geometry can be effectively used for characterizing the surface texture formed during machining. A significant finding in this study is that the fractal dimension calculated using the optical area-based method is less sensitive to changes in the optical parameters in the measurement system and has its unique capability of detecting variation in the surface texture occurred during the machining operation.

An analysis of variance is performed using the data listed in Table 2. The four specimens with their known roughness average values are viewed as four treatments. The differences between the four means of fractal dimension can be contributed by the variation of machining conditions used to prepare the four specimens. If examining the variation of fractal dimension within each of the four columns, the variation is caused by the variation of the optical parameters in the measurement system. Table 3 is an analysis of variance table listing the two sources of variation. They are 0.333 for the machining condition variations (3 degrees of freedom) and 0.0873 for the optical parameter variation (60 degrees of freedom), respectively. The ratio of these two mean squares, $\frac{0.333/3}{0.087/60} = 76$, is a strong indication that, from statistical viewpoint, real differences exist among the four specimens in terms of using the fractal dimension representation even at the presence of noise introduced by the measurement system. The noise is usually unavoidable in practice.

4.3 Limitations of the Prototype System

(a) System calibration

As indicated in the sensitivity analysis, the system calibration should be performed under machining conditions as similar to the actual machining operation as possible. Deviations in the calibration conditions from the actual machining operation can lead to failure of detecting deterioration of surface finish or false alarms during the on-line monitoring. At this stage of research, a new calibration curve is constructed when machining and environmental conditions change. A typical example would be a change in the workpiece material due to the variation of optical properties of the material being machined.

(b) Maximum feedrate for reliable operation

The quality of image data relies on the frame grabber speed. The current video acquisition systems usually use interlace scanning to obtain the image. When the frame grabber speed is not compatible with the moving speed of the object, double images may be formed, and the prototype system is not capable of making corrections. Currently the maximum feedrate used by the prototype system is 254 mm/min.

5. CONCLUSIONS

In this study, a prototype system is developed to perform surface roughness measurements using an area based fractal approach. This approach makes it especially suitable for on-line process monitoring. A functional calibration curve which relates the fractal dimension to the surface roughness is constructed in this study. The close correlation between the fractal dimension and roughness average shows that the developed system provides an effective method for surface characterization during machining. A significant finding in this study is that the calculated fractal dimension is sensitive enough to detect the variation in the surface finish even with the presence of variation in ambient conditions. The challenge in implementing this system is that the calibration process has to be done under the similar conditions that exist in the machining environment. Research in this area is still in progress to search for systems more practical in the industrial environment.

ACKNOWLEDGMENTS

The authors acknowledge the support of the University of Maryland Research Board, the Department of Mechanical Engineering, and the Institute for Systems Research at the University of Maryland under Engineering Research Centers Program: NSFD CDF 8803012. They also wish to express their gratitude for the assistance provided by Mr. J. F. Song of National Institute of Standards and Technology.

REFERENCES

1. S. Vandenberg and C.F. Osborne, “Digital image processing techniques, fractal dimensionality and scale-space applied to surface roughness”, *Wear*, Vol. 159, 17-30 (1992).
2. R. Thwaite, "The numerical interpretation of topography," *Wear*, Vol. 51, 253-267 (1978).
3. D. Gilsinn, T. Vorburger et al., “Optical Roughness Measurements of Industrial Surfaces”, *Optical Techniques for Industrial Inspection*, Vol. 665, 231-238 (1978).

4. A. Majumdar and C.L.Tien, "Fractal characterization and simulation of rough surfaces", *Wear*, Vol. 136, 313-327 (1990).
5. A. Majumdar and B. Bhushan, "Role of Fractal Geometry in Roughness Characterization and Contact Mechanics of Surfaces", *Journal of Tribology*, Vol. 112, 205-216 (1990).
6. F. Ling, "Fractals, engineering surfaces and tribology", Wear, 136, 141-156 (1990).
7. D. DeVoe, L. Knox, and G. Zhang, 1992, "Active control of Machining Processes Using Image Reconstruction and Processing", *Proceedings of Thirteenth Annual Allerton Conference on Communication, Control and Computing*, Sep. 30 - Oct. 2, 742-750 (1992).
8. D. DeVoe, "Optical Area based Surface Quality Assessment for In-Process Measurement", *M.S. Thesis*, University of Maryland, College Park (1993).
9. B. Mandelbrot, *Fractal Geometry of Nature*, W.H. Freeman, New York (1982).
10. R. Barnsley and R. Devaney, *The Science of Fractal Images,* Springer-Verlag, New York (1988).
11. B. Mandelbrot, "Self-affine fractals and the fractal dimension", *Physics Scripta* , Vol. 32, 257-260 (1985).
12. T. Thomas, *Rough Surfaces* , Longman Inc., New York (1982).
13. L. Liebovitch and T. Toth, "A Fast Algorithm to determine Fractal Dimension by Box Counting", *Physics Letters A,* volume 141, number 8,9, 386-390 (1989).
14. G. Box, W. Hunter, and J. Hunter, *Statistics for experimenters*, John Wiley & Sons (1978).

List of Figures

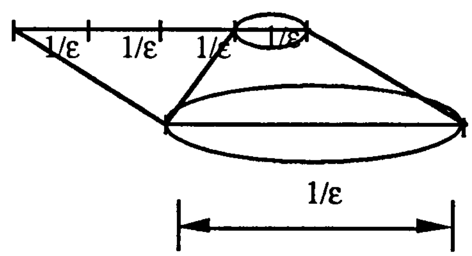

(a) Segment of length 1/ε magnified by ε resulting in the original line

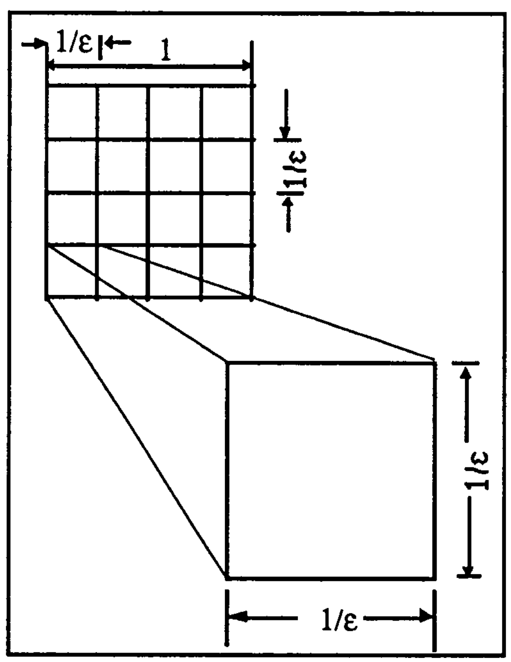

(b) Small square of side 1/ε magnified by ε resulting in the original square

Figure 1 Concept of self-similarity

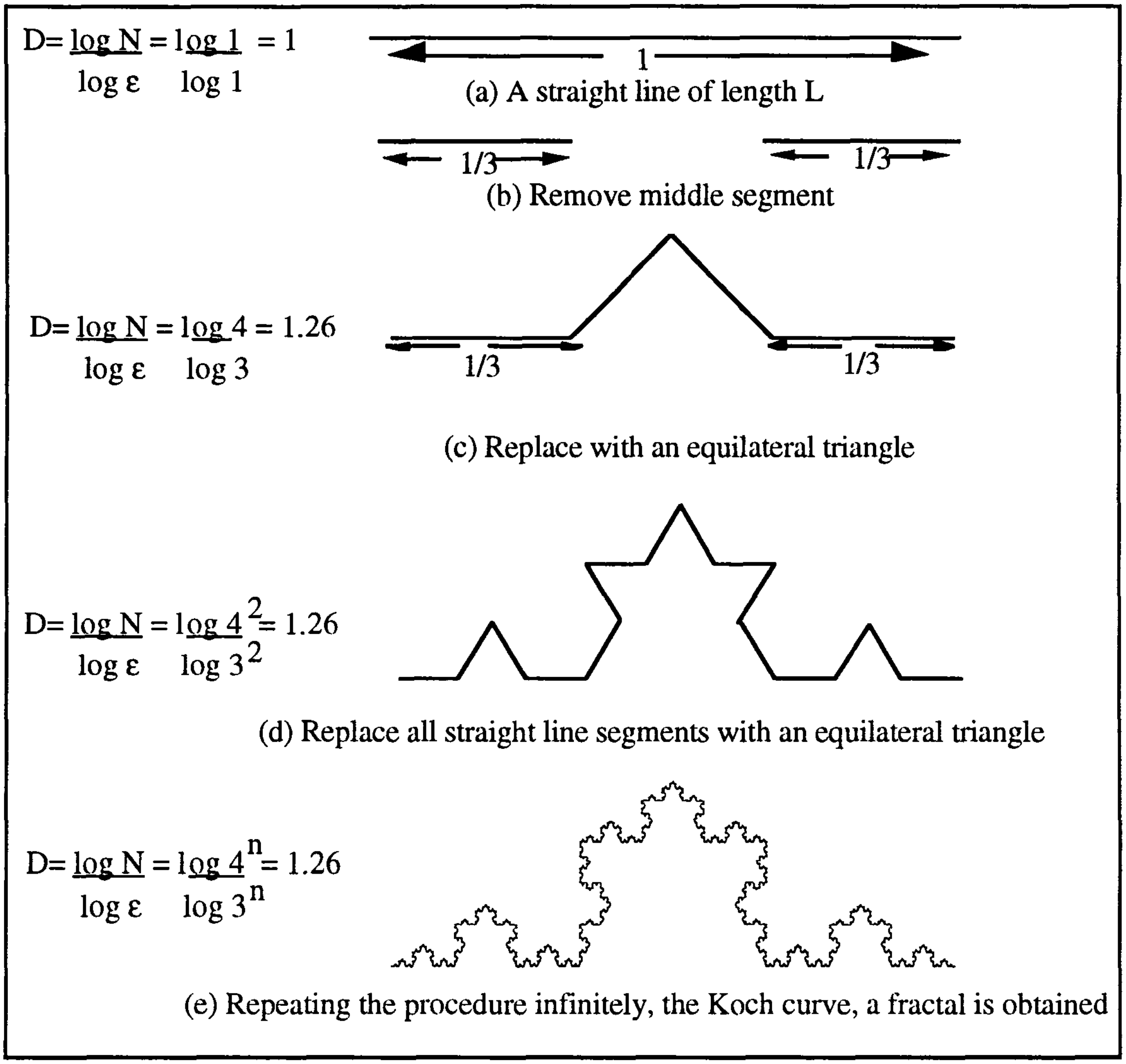

Figure 2 Construction of Koch curve

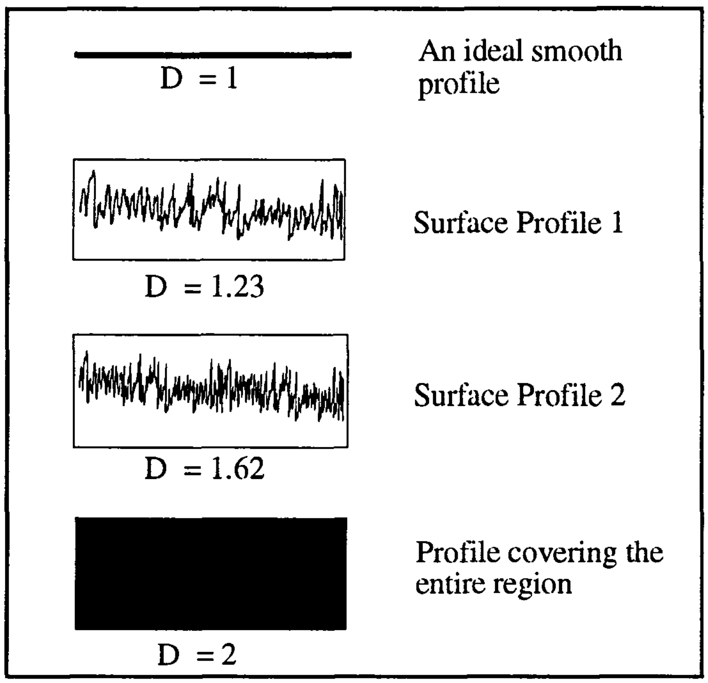

Figure 3 Fractal geometry applied to surface finish estimation

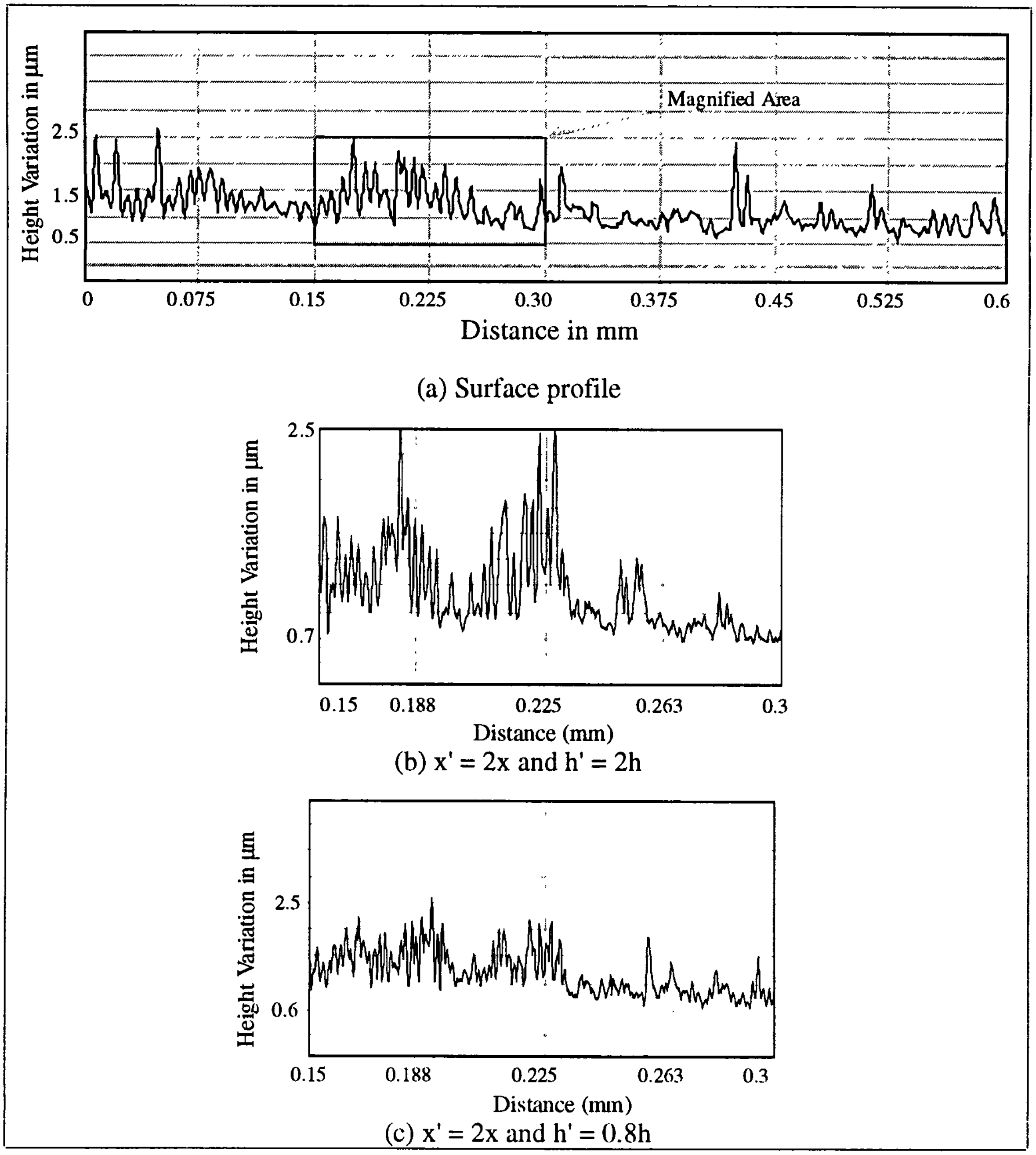

Figure 4 Surface profile under different magnification scales on the x and h axes

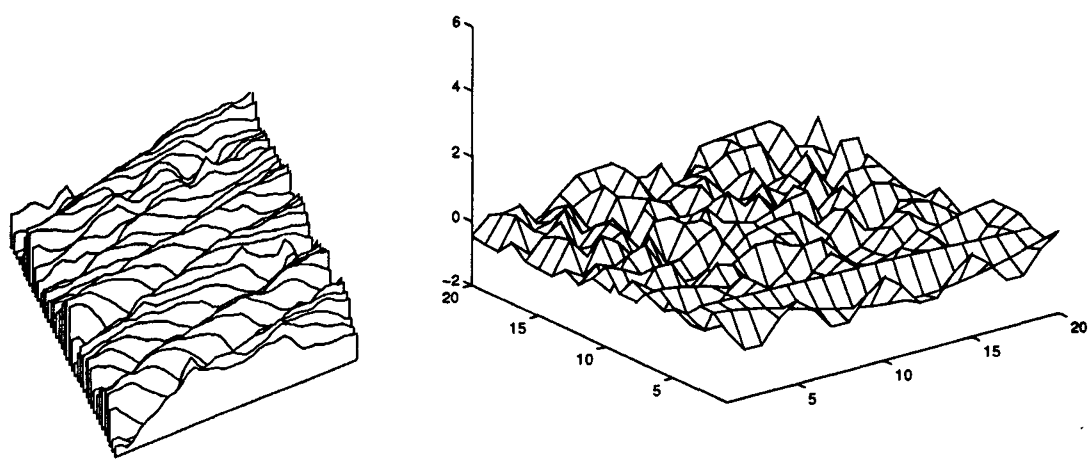

Surface topography

Simulated surface topography

Figure 5 Actual topography and surface topography generated using W-M function

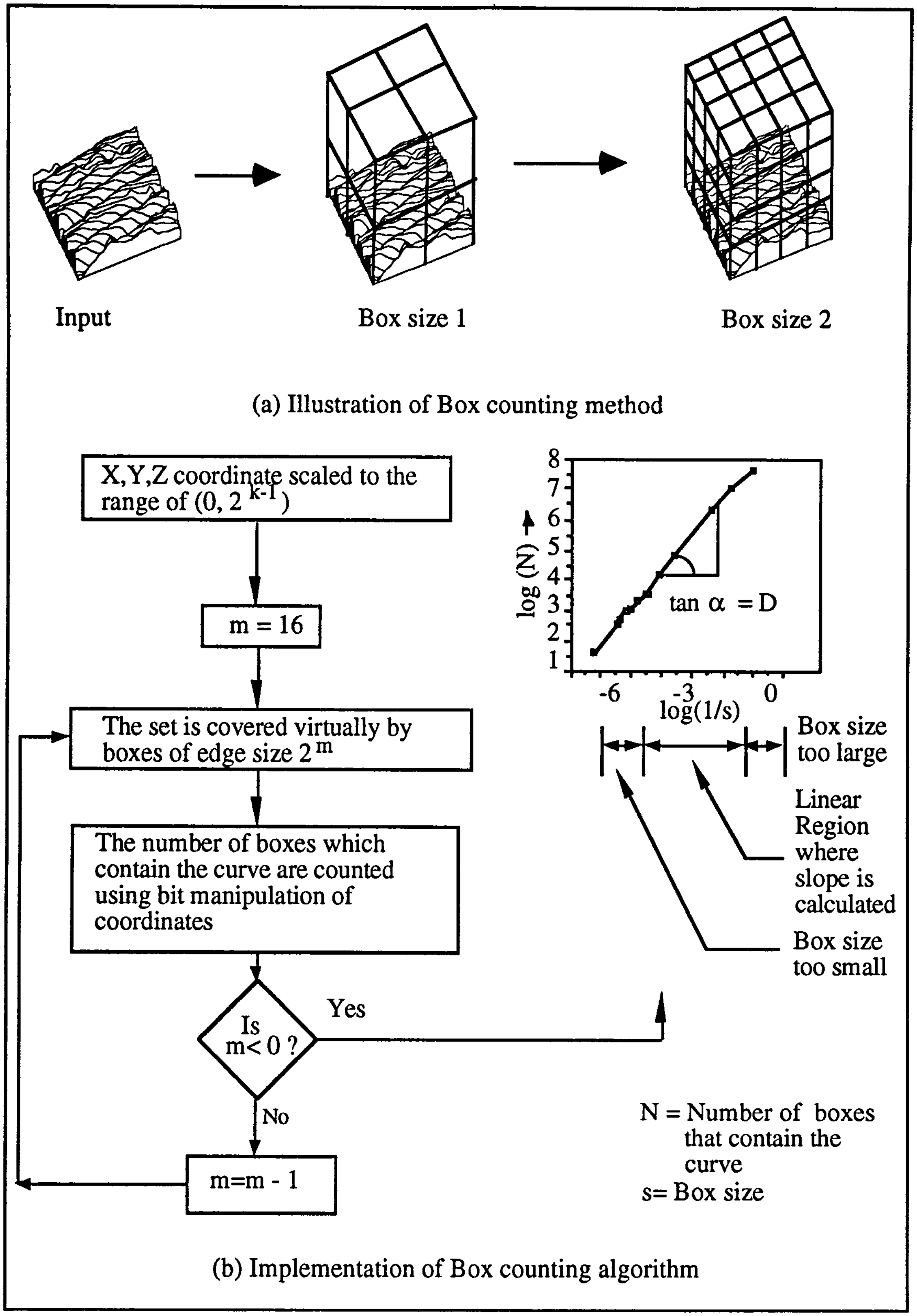

(a) Illustration of Box counting method

(b) Implementation of Box counting algorithm

Figure 6 Box counting method to estimate fractal dimension

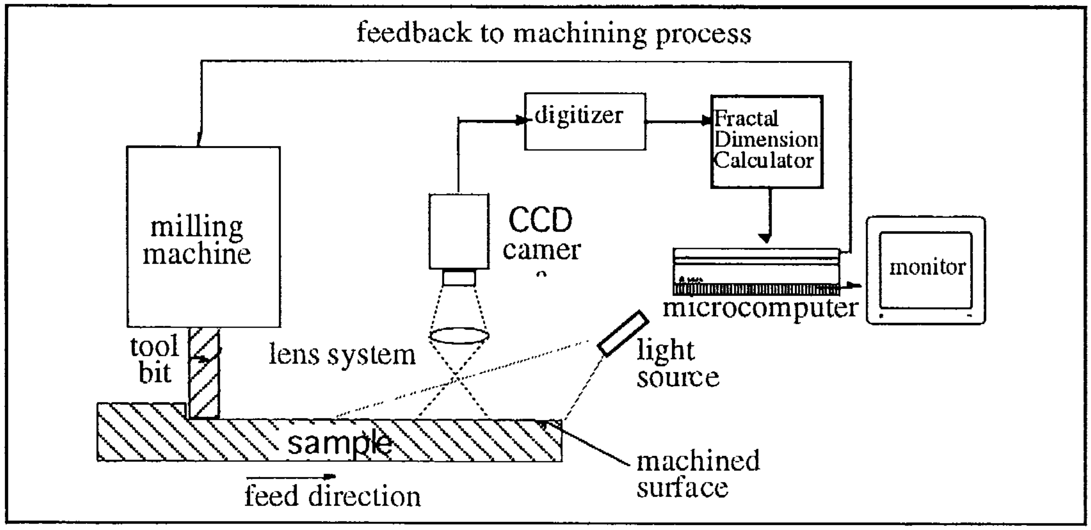

(a) Basic components of the prototype system

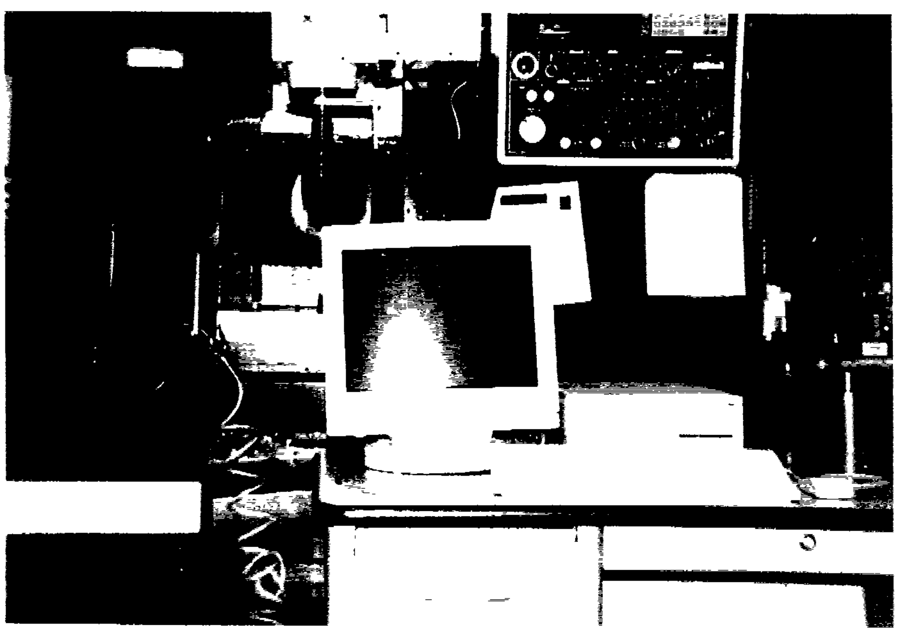

(b) Implementation on a CNC machining center

Figure 7 Design and implementation of the prototype system

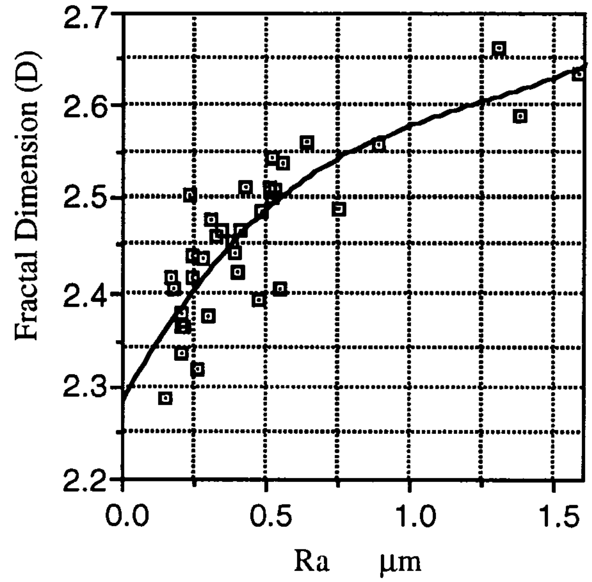

(a) Correlation curve between Fractal Dimension and Ra

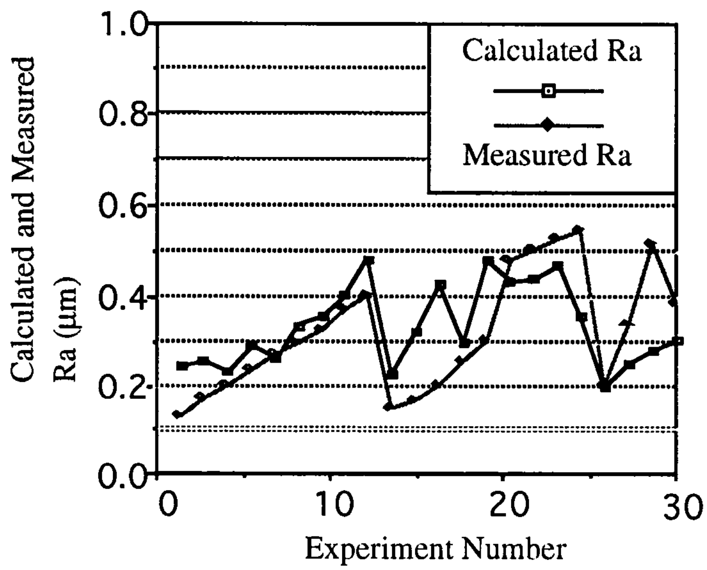

(b) Comparison of estimated and measured Ra values

Figure 8 Results from implementation on the CNC machining center.

List of Tables

Table 1 Factorial Design with Four Variables at Two Levels

Factors under Investigation	High Level (+)	Low Level (-)
Horizontal orientation of light (O.L.)	55°	45°
Incident angle of light (I.A.)	20°	10°
Light source intensity (L.I.)	100%	80%
Ambient lighting (A.L.)	off	on

Table 2 Fractal Dimensions Calculated from the Factorial Experimental Data

	O.L	I.A	L.I	A.L	Specimen 1	Specimen 2	Specimen 3	Specimen 4
1	-	-	-	-	2.3251	2.2505	2.2179	2.1258
2	+	-	-	-	2.3760	2.3046	2.2626	2.1523
3	-	+	-	-	2.3566	2.2845	2.2498	2.1679
4	+	+	-	-	2.4036	2.3363	2.2928	2.1889
5	-	-	+	-	2.3918	2.2999	2.2746	2.1922
6	+	-	+	-	2.4241	2.3392	2.3038	2.2129
7	-	+	+	-	2.4045	2.3383	2.2889	2.2134
8	+	+	+	-	2.4521	2.3769	2.3273	2.2255
9	-	-	-	+	2.4171	2.3493	2.2983	2.2529
10	+	-	-	+	2.4333	2.3611	2.3086	2.2545
11	-	+	-	+	2.4182	2.3589	2.2932	2.2553
12	+	+	-	+	2.4736	2.3680	2.3108	2.2603
13	-	-	+	+	2.4365	2.3595	2.3050	2.2462
14	+	-	+	+	2.4559	2.3780	2.3175	2.2494
15	-	+	+	+	2.4415	2.3670	2.2991	2.2533
16	+	+	+	+	2.4736	2.3892	2.3248	2.2638
				Mean	2.4177	2.3413	2.2921	2.2196
				Std. Dev	0.0409	0.0382	0.0288	0.0430
Measured Ra (μm)					0.70	0.53	0.36	0.23

Table 3 Results from the F-Test

Source of variation	Sum of Squares	Degree of Freedom	Mean Square	Ratio
Average	343.8	1	343.8	
Between Treatments	0.333	3	0.111	$\frac{\frac{0.333}{3}}{\frac{0.087}{60}} = 76.3$
Within Treatments	0.087	60	0.00145	
Total	344.22	64		